Nanocomposite field effect transistors based on zinc oxide/polymer blends

Zong-Xiang Xu and V. A. L. Roy[a),b)]
Department of Chemistry and HKU-CAS Joint Laboratory on New Materials, The University of Hong Kong, Pokfulam Road, Hong Kong Special Administrative Region, Hong Kong

Peter Stallinga
Universidade do Algarve, 8005–139 Faro, Portugal

Michele Muccini and Stefano Toffanin
CNR-ISMN, Istituto per lo Studio dei Materiali Nanostrutturati, 40129 Bologna, Italy

Hei-Feng Xiang and Chi-Ming Che[a),c)]
Department of Chemistry and HKU-CAS Joint Laboratory on New Materials, The University of Hong Kong, Pokfulam Road, Hong Kong Special Administrative Region, Hong Kong

(Received 15 November 2006; accepted 24 April 2007; published online 1 June 2007)

The authors have examined the field effect behavior of nanocomposite field effect transistors containing ZnO (zinc oxide) tetrapods or nanocrystals dispersed in a polymer matrix of poly[2-methoxy,5-(2-ethylhexyloxy)-1,4-phenylenevinylene] (MEH-PPV). The electrical characteristics of ZnO tetrapods/MEH-PPV composite devices exhibit an increase in hole mobility up to three orders of magnitude higher than the polymer MEH-PPV device. © *2007 American Institute of Physics*. [DOI: 10.1063/1.2740478]

Nanocomposite materials are of growing interest particularly for their potential practical applications in various electronic devices, especially light-emitting diodes and photovoltaics.[1] Despite these advances, using nanocomposite materials for organic field-effect transistor (OFET) applications remain scarce. OFETs have been recently reported in the fabrication of active-matrix displays and integrated circuits for logic and memory chips.[2] Even though numerous reports exist in this area, OFET devices based on nanocomposite materials fabricated using solution processing are still not well known. In this context, dispersing nanomaterials in a polymer matrix to obtain solution processed devices with a high mobility is of interest for both basic research and application.

In this work, we dispersed ZnO nanocrystals or tetrapods in the poly[2-methoxy,5-(2-ethylhexyloxy)-1,4-phenylene vinylene] (MEH-PPV) polymer matrix for the construction of inorganic/organic hybrid devices for OFET applications. We chose ZnO nanomaterials and MEH-PPV polymer because these two materials are widely studied for their intriguing optoelectronic properties.[3] In literature, there have been reports on inorganic tetrapods mixed with polymers to fabricate hybrid photovoltaic devices.[4] Herein, the electrical properties of solution processed MEH-PPV ZnO nanocomposite devices have been found to have enhanced *p*-type mobility up to three orders of magnitude higher than the polymer MEH-PPV device.

The ZnO nanocrystals were prepared via a modified Pacholski's method.[5] An ethanol solution of sodium hydroxide (NaOH) (0.3 M, 20 ml) was slowly added to a solution of zinc (II) nitrate hexahydrate $Zn(NO_3)_2 \cdot 6H_2O$ in ethanol (0.3 M, 10 ml) at 0 °C which was vigorously stirred for 2 h, and subsequently heated further for 2 h. A precipitate of nanocrystals was obtained, which was washed with ethanol and toluene.

ZnO tetrapods were synthesized according to a procedure described in Ref. 6. In a typical synthesis, about 0.5 g of pure Zn (99.99%) was kept in an alumina boat as a source material. Later the source was transferred into a long quartz tube. A tube furnace with the temperature ramped up to 1000 °C at a rate of ~50 °C/min was used for chemical vapor deposition and the tube furnace was kept at 1000 °C for more than 20 min under a constant flow of nitrogen and oxygen mixture (1:1). The ZnO tetrapods were formed by moving the quartz tube inside the tube furnace to place the alumina boat with the source at the heating center (1000 °C) for around 20 min. After the furnace was cooled to room temperature, the ZnO tetrapods were removed.

A number of different nanocomposites have been made that contained ZnO nanocrystals or tetrapods dispersed in the polymer matrix, MEH-PPV. In this work, the nanocomposites which contained polymer with nanocrystals or terapods were made in various conditions with the following weight proportions: 10 mg of polymer to *X* mg of ZnO tetrapods or nanocrystals where $X=1$, 3, 5, 7, 9, and 10. Therefore, the weight percentage of ZnO in MEH-PPV polymer in these devices are 9%, 23%, 33%, 41%, 47%, and 50% respectively. The ZnO tetrapods or nanocrystals were dispersed in a toluene solution of MEH-PPV (molecular weight of 500 000 from H.W. Sands Co.) using an ultrasonic bath.

The transistors were fabricated on bottom-gate transistor structure with a spin coated ZnO/polymer nanocomposite thin film as active layer. Gate oxide SiO_2 layer (100 nm, relative permittivity=3.9) was thermally grown on heavily doped *n*-type Si substrates (the gate electrode). An image reversal photolithography technique was used to form an opening on the photoresist layer for the source and drain patterns on the gate oxide. Source and drain metal layers, consisting of Ti adhesion film (10 nm, lower) and Au conductive film (50 nm, upper), were deposited by thermal evaporation. After metal film deposition, a standard lift-off

a)Authors to whom correspondence should be addressed.
b)Electronic mail: valroy@hku.hk
c)Electronic mail: cmche@hku.hk

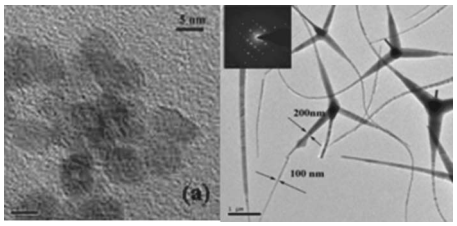

FIG. 1. TEM images of (a) ZnO nanocrystals and (b) ZnO tetrapods dispersed in MEH-PPV [the inset picture shows a selected area electron diffraction (SAED) pattern of tetrapods].

process in acetone was used to remove the metal film on top of the photoresist pattern, leaving behind the Ti/Au source/drain contact patterns. The transistor output and transfer characteristics were measured with a probe station under a nitrogen atmosphere using a Keithley K4200 semiconductor parameter analyzer. The transistor channel length and widths were 10 and 600 μm, respectively.

The fabricated devices that contained a layer of MEH-PPV only exhibited *p*-channel behavior with a hole mobility up to 10^{-4} cm^2/V s, similar to those previously reported.[3] Figures 1(a) and 1(b) show the transmission electron microscope (TEM) images of ZnO nanocrystals or tetrapods dispersed in MEH-PPV solutions, respectively. The size of the nanocrystals is around 5 nm [Fig. 1(a)] and the legs of the tetrapods are around 100 nm in width [Fig. 1(b)]. Figure 2 shows the electrical behavior of the devices fabricated from MEH-PPV and nanocomposite with ZnO nanocrystals or tetrapods. In Fig. 2, the *I-V* characteristics and the transfer curves of the devices based on MEH-PPV [Figs. 2(a) and 2(b)] 9 mg of ZnO nanocrystals in 10 mg of MEH-PPV or 47% of ZnO in weight [Figs. 2(c) and 2(d)] and 9 mg of ZnO tetrapods in 10 mg of MEH-PPV or 47% of ZnO in weight [Figs. 2(e) and 2(f)], are depicted. A saturation of the hole mobility is observed in the nanocomposite devices when the concentration of ZnO tetrapods or nanocrystal exceeds 40% in weight, as shown in Fig. 3. From the *I-V* characteristics, incorporation of ZnO nanocrystals or tetrapods in the polymer enhances the drain current and the mobility. The calculated hole mobility was up to 0.08 cm^2/V s for the ZnO

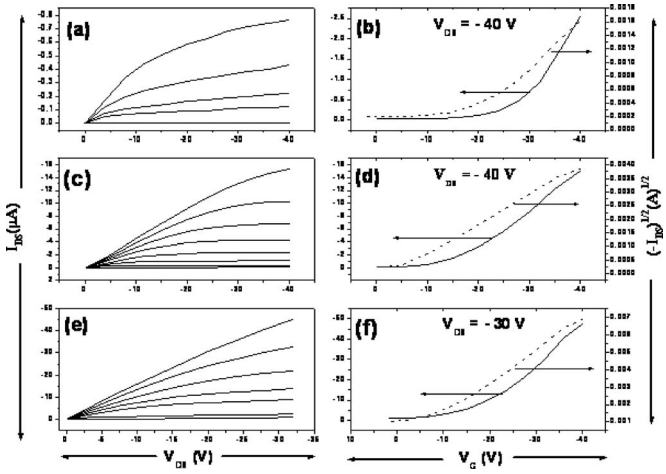

FIG. 2. *I-V* characteristics and the transfer curves for devices containing MEH-PPV [(a) where V_{GS}=0, −25 to −40 V in steps of 5 V and (b) where V_{DS}=−40 V], 9 mg of nanocrystals in 10 mg of MEH-PPV [(c) where V_{GS}=0 to −40 V in steps of 5 V and (d) where V_{DS}=−40 V], and 9 mg of ZnO tetrapods in 10 mg of MEH-PPV [(e) where V_{GS}=0 to −30 V in steps of 5 V and (f) where V_{DS}=−30 V], respectively.

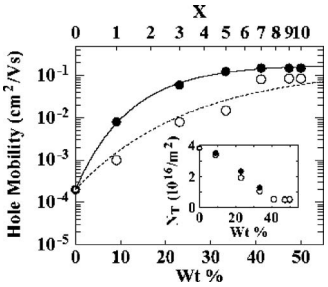

FIG. 3. Correlation between the mobility and the concentration of ZnO in the form of nanocrystals (solid circles) or tetrapods (open circles) in MEH-PPV. The lines are guides to the eye. The inset shows the density of traps as a function of ZnO concentration, calculated on basis of the found threshold voltage, $N_T=-V_T\ C_{ox}/q$. We propose that the increased mobility is mainly due to the reduction of traps in MEH-PPV.

nanocrystals/MEH-PPV devices and up to 0.15 cm^2/V s for the ZnO tetrapods/MEH-PPV devices, at the saturation regime. Whereas in the linear regime, the hole mobility was up to 0.071 cm^2/V s for the ZnO nanocrystals/MEH-PPV devices and up to 0.096 cm^2/V s for the ZnO tetrapods/MEH-PPV devices. A decrease in the threshold voltage up to −15 V was found for both nanocomposite devices (ZnO nanocrystals or ZnO tetrapods/MEH-PPV). The subthreshold swing was found to be 2 V/decade for the ZnO/MEH-PPV nanocomposite devices and up to 10 V/decade for the MEH-PPV devices. The on/off ratio was calculated as 10^5 for the nanocomposite devices where it was only 10^3 for MEH-PPV devices. Furthermore, a reduction in density of traps, given by $N_T=-V_TC_{ox}/q$, has been observed, as shown in the inset of Fig. 3, while the weight percentage of ZnO increases in the polymer. However, the trap density seems to saturate when the concentration of ZnO tetrapods or nanocrystal in the polymer exceeds 40% in weight.

Incorporation of ZnO nanomaterials (nanocrystals or tetrapods) into the MEH-PPV polymer—a *p*-type semiconductor—did not change the nature of charge transport, as the nanocomposite devices were found to behave as *p*-channel transistors. However, the hole mobility was enhanced in the nanocomposite devices. We also fabricated ZnO tetrapod devices, containing only ZnO tetrapods, by drop casting the solution of ZnO tetrapods dispersed in ethanol on a bottom contact device. The aggregated tetrapods exhibited ambipolar behavior (Fig. 4, available at supplementary information[7]) as evidenced from their electrical characteristics in which case the current increased at higher gate voltages in both positive and negative drain-source voltages. Since a clear saturation was not observed in both the positive and negative gate biases, the charge mobility was calculated from the linear regime and it was found to be 10^{-3} cm^2/V s for holes. This value is lower than the ZnO tetrapods/MEH-PPV composite devices. Moreover, no electron current was observed in these composite devices. This indicates that charge transport takes place only in the MEH-PPV polymer. In addition, the energy diagrams of MEH-PPV and ZnO are well known. The highest occupied molecular orbital (5.3 eV) and lowest unoccupied molecular orbital (3.0 eV) levels of MEH-PPV and the valence (7.6 eV) and conduction (4.4 eV) bands of ZnO show clearly that a huge energy barrier exists for holes to be transferred from ZnO to MEH-PPV for transport.[8] Consequently, holes are confined in MEH-PPV and we suggest that the effect of ZnO is to reduce the density of traps in the

polymer which probably is a reason for the enhanced mobility and the reduced threshold voltage.

Photoluminescence (PL) measurements were done for ZnO tetrapods, MEH-PPV, and ZnO tetrapods/MEH-PPV composite films (Fig. 5, available at supplementary information[7]). The PL measurements explained that the surface state green emission from the ZnO tetrapods was quenched in the composite film. This suggests that the polymer MEH-PPV covered the surface of ZnO tetrapods; the latter were distributed randomly in the MEH-PPV polymer matrix. The nonaggregated and nonoriented (random) distributions of ZnO tetrapods in MEH-PPV matrix have also been observed from the TEM image [Fig. 1(b)]. Hysteresis measurements [Figs. 6(a) and 6(b), available at supplementary information[7]], a close loop measurement by scanning V_{GS} from 0 to −40 V and back to 0 V with constant drain-source voltage, for both MEH-PPV and ZnO tetrapods/MEH-PPV composite devices have been undertaken in this work. Since the backward curve falls below the forward one there is an increase in threshold voltage during operation of the MEH-PPV device. The MEH-PPV device significantly exhibited more hysteresis effect than the ZnO tetrapods/MEH-PPV composite devices. In literature, there are several reports revealing that the planar charge transport and charge mobility of OFET devices are affected by the presence of "traps" in the organic semiconductors.[9] In this work, we did transient measurements where a constant voltage was applied to the gate and drain (−30 V), while the current was measured as a function of time on the MEH-PPV and ZnO tetrapods/MEH-PPV devices. The results are depicted in Fig. 7 at the supplementary information[7]. The decrease in the channel current with time is much more dramatic for the MEH-PPV than for the ZnO tetrapods/MEH-PPV devices. This finding, together with considerably less hystersis effects observed for the composite device depicted in Fig. 6(b), suggests that trapping is reduced in the ZnO tetrapods/MEH-PPV devices. We suggest that a reduction of the density of traps (Fig. 3) is probably the reason for the increased performance of the devices.[10] The nanocomposite devices with high ZnO concentration (ZnO tetrapod to polymer weight ratio above 5:10) were found to be stable for more than a month.

In summary, we have fabricated ZnO/MEH-PPV based nanocomposite devices with enhanced *p*-channel FET characteristics by a simple solution processing approach. Devices containing various concentrations of ZnO nanomaterials (tetrapods and nanocrystals) in MEH-PPV were fabricated and analyzed. This revealed that incorporation of ZnO nanomaterials into the polymer matrix enhances the hole mobility of the devices by up to three orders of magnitude. For the ZnO nanocrystals/MEH-PPV composite device, the hole mobility is up to 0.08 $cm^2/V\,s$ and for ZnO tetrapods/MEH-PPV composite device is up to 0.15 $cm^2/V\,s$. We note that current hysteresis was significantly reduced in ZnO tetrapods/MEH-PPV composite devices in contrast to the hysteresis effect observed for the MEH-PPV devices.

This work was supported by the Joint Research Scheme NSFC/RGC (N_HKU 742/04) and University Development Fund (Nanotechnology Research Institute, 00600009) of The University of Hong Kong. Support from Hung Hing Ying funding, HKU [see funding (200511159003)], ITF (GHP/062/05), Italian MIUR Project (FIRB-RBNE033KMA), Portuguese POCTI/FAT/47956/2002, and Strategic theme on organic opto-electronics is gratefully acknowledged.

[1] C. Sanchez, B. Julian, P. Belleville, and M. Popall, J. Mater. Chem. **15**, 3559 (2005); W. J. E. Beek, M. M. Wienk, and R. A. J. Janssen, Adv. Mater. (Weinheim, Ger.) **16**, 1009 (2004); C. Melzer, E. J. Koop, V. D. Mihailetchi, and P. W. M. Blom, Adv. Funct. Mater. **14**, 865 (2004).

[2] B. Comiskey, J. D. Albert, H. Yoshizawa, and J. Jacobson, Nature (London) **394**, 253 (1998); J. M. L. Chabinyc and A. Salleo, Chem. Mater. **16**, 4509 (2004).

[3] R. F. Service, Science **276**, 895 (1997); T. Aoki, Y. Hatanaka, and D. C. Look, Appl. Phys. Lett. **76**, 3257 (2000); H. Ohta, K. Kawamura, M. Orita, M. Hirano, N. Sarukura, and H. Hosono, *ibid.* **77**, 475 (2000); R. L. Hoffman, B. J. Norris, and J. F. Wager, *ibid.* **82**, 733 (2003); B. J. Norris, J. Anderson, J. F. Wager, and D. A. Keszler, J. Phys. D **36**, L105 (2003); E. J. Meijer, D. M. Deleeuw, S. Setayesh, E. Vanveenendaal, B. H. Huisman, P. W. M. Blom, J. C. Hummelen, U. Scherf, and T. M. Klapwijk, Nat. Mater. **2**, 678 (2003); L. L. Chua, J. Zaumseil, J. F. Chang, E. C. W. Ou, P. K. H. Ho, H. Sirringhaus, and R. H. Friend, Nature (London) **434**, 194 (2005).

[4] B. Sun, E. Marx, and N. C. Greenham, Nano Lett. **3**, 961 (2003).

[5] C. Pacholski, A. Kornowski, and H. Weller, Angew. Chem., Int. Ed. **41**, 1188 (2002).

[6] V. A. L. Roy, A. B. Djurišić, W. K. Chan, J. Gao, H. F. Lui, and C. Surya, Appl. Phys. Lett. **83**, 141 (2003).

[7] See EPAPS Document No. E-APPLAB-90-067720 for the supplementary information. This document can be reached via a direct link in the online article's HTML reference section via the EPAPS homepage (http://www.aip.org.pubservs.epaps.html).

[8] A. Hagfeldt and M. Gratzel, Chem. Rev. (Washington, D.C.) **95**, 49 (1995).

[9] P. Stallinga, H. L. Gomes, F. Biscarini, M. Murgia, and D. M. J. Leeuw, J. Appl. Phys. **96**, 5277 (2004); V. Podzorov, E. Menard, A. Borissov, V. Kiryukhin, J. A. Rogers, and M. E. Gershenson, Phys. Rev. Lett. **93**, 086602 (2004).

[10] P. Stallinga and H. L. Gomes, Synth. Met. **156**, 1305 (2006).